Cellulose (2024) 31:235–246
https://doi.org/10.1007/s10570-023-05607-9

ORIGINAL RESEARCH

Effect of aziridino[60]fullerenes on thermal stability of nitrocellulose

Jie Xiong · Shuang Feng · Rufang Peng · Bo Jin

Received: 24 May 2023 / Accepted: 9 November 2023 / Published online: 9 December 2023

Abstract A series of aziridino[60]fullerenes was synthesized by the reaction of octabromo[60]fullerene with various anilines. Their ability to absorb free radicals and acid gases was studied, and their potential applications as stabilizers in nitrocellulose-containing propellants were discussed. The results of differential thermal analysis showed that aziridino[60]fullerene can increase the exothermic peak temperatures of nitrocellulose by 0.55–2.37 °C. The methyl violet test found that aziridino[60]fullerenes can extend the complete decomposition period by 31–71 min. The results of vacuum stability test and thermogravimetric test indicated that aziridino[60]fullerene can delay the decomposition of nitrocellulose. Furthermore, their stabilization mechanism was studied by electron spin resonance spectroscopy, and the free-radical scavenging rate of **3c** reached 86.09%. The findings demonstrate that aziridino[60]fullerenes could effectively eliminate the nitrogen oxides released by nitrocellulose autocatalysis and might be used as a new stabilizer for nitrocellulose-containing propellants.

Jie Xiong and Shuang Feng have contributed equally to this work and should be considered co-first authors.

Supplementary Information The online version contains supplementary material available at https://doi.org/10.1007/s10570-023-05607-9.

J. Xiong · S. Feng · R. Peng (✉) · B. Jin (✉)
State Key Laboratory of Environment-Friendly Energy Materials, Southwest University of Science and Technology, Mianyang 621010, Sichuan, China
e-mail: rfpeng2006@163.com

B. Jin
e-mail: jinbo0428@163.com

Graphical abstract

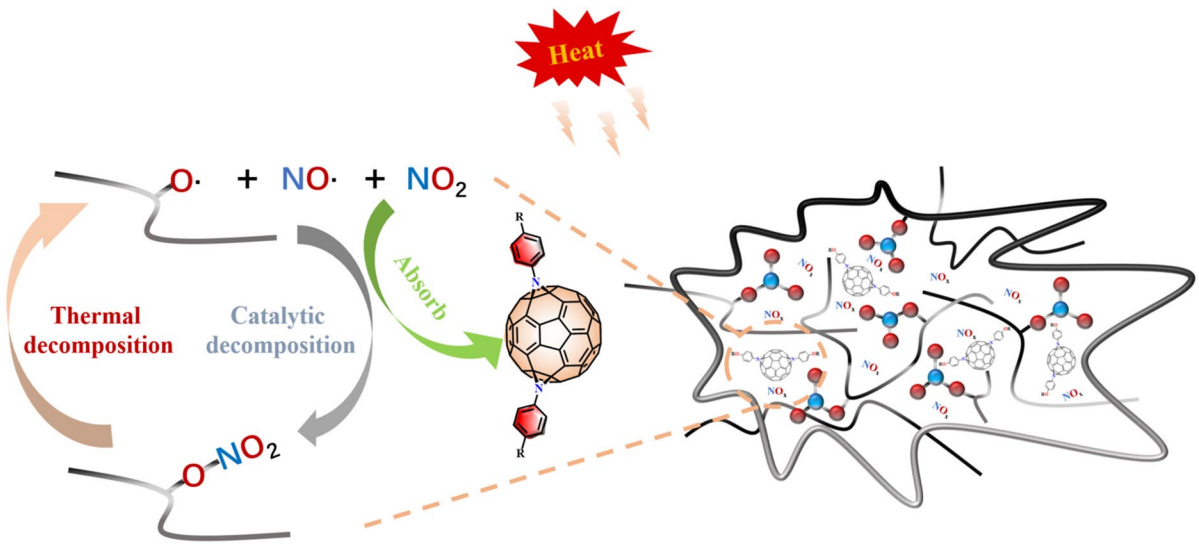

Keywords Fullerene · Nitrocellulose · Stability · Propellant · Mechanism

Introduction

Solid propellant is a kind of energetic composite material that plays an important role in the development of missiles and aerospace technology (Sabri et al. 2023; Luo et al. 2019b, a; Nassima et al. 2022). Usually, it could be divided into double-base propellant, composite propellant (Bagalkote et al. 2018), and modified double-base propellant (Elbasuney et al. 2018). Double-base propellant contains a large number of nitrate esters such as nitrocellulose (NC) and nitroglycerin (NG). The activation energy of O–NO_2 bond breaking is about 167 kJ/mol, and the thermal sensitivity is high, which could reduce the initiation energy and improve the detonation performance of the propellant. Additionally, due to its noteworthy qualities, including excellent mechanical characteristics, good solubility, compatibility with a variety of additives, rapid drying rate, flammability, and explosiveness, it has been widely used in the military and civil fields (Ahmed et al. 2023, 2020). However, during long-term storage, autocatalytic decomposition reactions are likely to occur under severe conditions, such as high temperature, moisture, and acid (Sabri et al. 2023; Salim et al. 2018; Zayed et al. 2017; Trache and Tarchoun 2019; Zhao et al. 2007). The nitroxyl radicals and acid gases produced by thermolysis promote the autocatalytic decomposition of nitrate esters, thus reducing the performance of the propellant and leading to burning or even explosion (Elbasuney et al. 2018; Trache and Tarchoun 2018; Luo et al. 2019b, a; Chai et al. 2019). A small number of chemical stabilizers could be added to absorb the nitrogen oxides to achieve the purpose of inhibiting autocatalytic decomposition to prolong the service life of solid propellants and explosives (Li et al. 2020a, b; Chelouche et al. 2019; Tang et al. 2017; Lindblom 2002; Lussier et al. 2000). The commonly used traditional stabilizers at present are mainly divided into anilines and phenylurea (Krumlinde et al. 2017; Wilker et al. 2007; Bohn 2009), such as diphenylamine (DPA), 2-nitrodiphenylamine (2-NDPA), *N*-methyl-*p*-nitro aniline (MNA), *N*,*N*′-diethyl-*N*,*N*′-diphenylurea (C1), *N*,*N*′-dimethyl-*N*,*N*′-diphenylurea (C2), 1,1-diphenylurea (AKI), and 3-methyl-1,1-diphenylurea (AKII) (Asthana et al. 1989a, b; Drzyzga 2003; Lussier et al. 2006; Asthana et al. 1989a, b). DPA, 2-NDPA, and MNA could absorb nitrogen–oxygen acid gases

through chemical reactions, inhibit the autocatalytic decomposition of NC, and improve the stability of propellants. However, the strong alkalinity of aniline stabilizer also promotes the saponification reaction of nitrate esters, which reduces the chemical stability of the propellant. Phenylurea stabilizers, such as C1, C2, AKI, and AKII, could reduce the alkalinity of the amine group due to the strong electron-withdrawing effect of the carbonyl group, which effectively delays the saponification, but weaken the ability to remove nitrogen–oxygen acid gas (Vennerstrom and Holmes, 1987; Purves et al. 1950; de Klerk 2015; Katoh et al. 2007). Recently, researchers have developed novel stabilizers such organosolv lignins and zeolites, but unlike amine compounds and urea compounds, they have not found any actual uses (Mohamed et al. 2020; Memdouh et al. 2023). However, most existing stabilizers cannot scavenge nitroxyl radicals. Therefore, we aim to prepare bifunctional stabilizers that can absorb both acid gases and nitroxyl radicals.

Fullerene is a zero-dimensional conjugated spherical molecule with excellent physical and chemical properties, including high thermal stability, oxidation resistance, and acid corrosion resistance (Proto 1997; Li et al. 2012; Montellano et al. 2011; Yan et al. 2016; McEwen et al. 1992). It is a sort of ideal material for the construction of chemical stabilizers, it could effectively remove various free radicals in the environmental system and have good compatibility with NC. [60]Fullerene is the only carbon material with a highly symmetrical structure in the fullerene family. In its 32-hedral structure, 60 carbon atoms are hybridized with $sp^{2.28}$, and each carbon atom provides an unhybridized p orbital. The side of the p orbital overlaps to form a non-planar conjugated delocalized large π system (Krusic et al. 1991; Taylor and Walton 1993; Closs et al. 1992). C_{60} can accept six electrons, demonstrating electron-deficient characteristics, and it has a great ability to absorb free radicals. The introduction of external groups could enhance the ability to scavenge free radicals through the chemical modification of fullerenes. Typically, Bingel, Prato, and F–C derivative methods were used to combine fullerenes with traditional stabilizers to design and synthesize a series of new fullerene cyclopropanes and pyrrolidines derivatives with dual-functional stability (Li et al. 2020a, b; Ding et al. 2019; Chai et al. 2020; Liao et al. 2021; Ishida et al. 2000; Jin et al. 2015). The thermal stability performance of fullerene-based materials to NC is better than that of DPA, C2, and other traditional stabilizers. Here, a series of aziridino[60]fullerenes synthesized by the nucleophile reaction of octabromo[60]fullerene $C_{60}Br_8$ with the corresponding *p*-alkyl aniline or *p*-alkoxy aniline was obtained according to our previous work (Xiong et al. 2023). The compatibility and stability of mono-adducted and *trans-4* bis-adducted aziridino[60] fullerenes to NC have been investigated for the first time, and their potential applicability as a stabilizer in double-base propellants was explored.

Experimental

Materials and characterization

All the substrates were purchased from Aladdin. The solvents were purchased from Kelong Chemical Reagents Corporation. C_{60} (purity > 99.9%) was obtained from Puyang Yongxin Fullerene Technology Corporation. Nitrocellulose samples with nitrate content (12.76% nitrogen) were supplied by the China Academy of Engineering Physics (Mianyang, Sichuan). Nuclear magnetic resonance (NMR) spectra were collected using a Bruker AVANCE III 600 MHz spectrometer, $CDCl_3$ and CS_2 as mixed solvents, and TMS as the internal standard. Fourier transform infrared spectroscopy (FT-IR) was recorded with a Nicolet-5700 FT-IR spectrometer using pressed KBr pellet in the range of 4000 cm^{-1} to 400 cm^{-1}. Ultraviolet–visible (UV–vis) spectra was recorded using a UV-1600 spectrophotometer with $CHCl_3$ as the solution. High resolution mass spectrometry (HRMS) was performed by MALDI-TOF in negative-ion mode with DCTB as the matrix. Data collection of single crystal was performed on a Smart Apex CCD diffractometer (Bruker) equipped with graphite monochromatism Cu Kα radiation ($\lambda = 1.54184$) using the ω and φ scan modes. A WCR-1B instrument under air atmosphere was used for differential thermal analysis (DTA). Vacuum stability test (VST) was executed by YC-1 from Xi'an Modern Chemistry Research Institute. Thermogravimetric (TG) analysis was undertaken with a 209 F1 model from NETZSCH of Germany. Free radical signal intensity was measured by electron spin-resonance spectroscopy with instrument of Bruker-EMX nano.

Scheme 1 Synthetic route of **2a-e** and **3a-c**

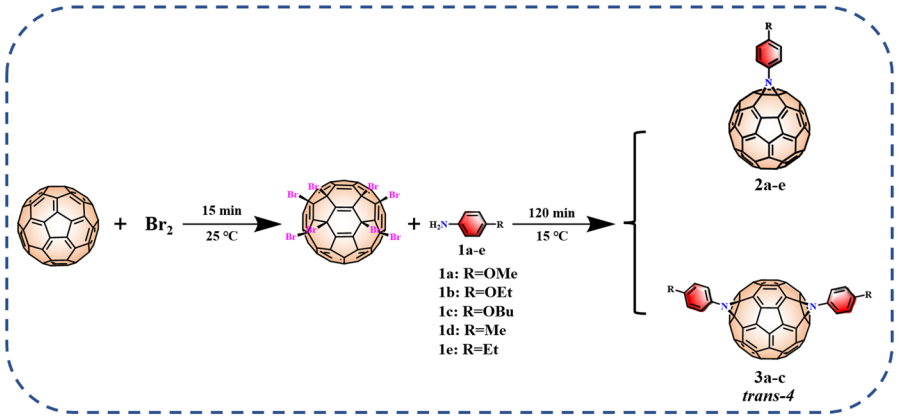

Table 1 Yields of **2a–e** and **3a–c**

Substrates	Products	Yield (%)
1a	**2a**	26
	3a	18
1b	**2b**	25
	3b	20
1c	**2c**	29
	3c	24
1d	**2d**	23
1e	**2e**	25

Table 2 Compositions of different nitrocellulose samples

Samples	Stabilizers	NC (wt%)	Stabilizers (wt%)
S-1	None	100	0
S-2	DPA	97	3
S-3	C2	97	3
S-4	**2a**	97	3
S-5	**2b**	97	3
S-6	**2c**	97	3
S-7	**2d**	97	3
S-8	**2e**	97	3
S-9	**3a**	97	3
S-10	**3b**	97	3
S-11	**3c**	97	3

Synthesis process

The synthetic route is shown in Scheme 1. C_{60} (200 mg) was added into a single-necked round-bottom flask. Then, 15 mL of Br_2 was poured, stirred, and reacted at room temperature for 15 min (Troshinn et al. 2003, 2004; Birkett et al. 1992; Xiao et al. 1994). After the reaction was completed, a sand core funnel was used for vacuum filtering, and the filtered solid was washed three times with saturated sodium bromide solution and distilled water to remove a small amount of Br_2 adsorbed on the surface. Finally, it was vacuum-dried to constant weight to obtain a bright black solid $C_{60}Br_8$ (365 mg, 97%).

Aziridino[60]fullerenes were synthesised according to previous work (Xiong et al. 2023). In detail, $C_{60}Br_8$ (200 mg, 0.1471 mmol) was placed in a 50 mL single-necked round bottom flask, added with 20 mL of toluene, and sonicated until it was dissolved. Then, **1a–e** (7.35 mmol) was added and stirred at room temperature for 120 min. After the reaction, the reaction solution was distilled under reduced pressure at 45 °C to remove toluene to obtain a brown–black oily liquid. Then, silica gel column separation by CS_2 was performed to obtain fuchsia solutions of mono-aziridino[60]fullerenes **2a–e** and bis-aziridino[60]fullerenes **3a–c**, illustrated in Scheme 1. The yields of **2a–e** and **3a–c** are shown in Table 1.

Methods of performance evaluation

The effects of aziridino[60]fullerenes on the thermal stability of nitrocellulose were investigated and contrasted with DPA and C2. Samples of NC/stabilizers containing different stabilizers were prepared using the solvent evaporation technique. In a nutshell, stabilizers (30 mg) were dissolved in 20 mL of carbon disulfide to form a homogenous system and which was added to a beaker containing 970 mg's NC subsequently. Then, the NC was dispersed in fullerene

derivatives solution and stirred magnetically for 1–1.5 h to acquire uniform blending mixes (NC/stabilizers). As the solvent evaporated spontaneously under ultrasonic, aziridino[60]fullerene well-proportioned disseminated over the NC surface. Finally, the mixes were dried for 48 h in a vacuum oven at 60 °C to get a uniform and dry combination, the composition of the base component was given in Table 2. Methyl violet, Differential thermal analysis (DTA), vacuum stability test (VST), and thermogravimetric (TG) analysis methods were applied to compare and evaluate the stability performance of aziridino[60] fullerene with DPA and C2.

Differential thermal analysis

DTA was applied to assess the thermal decomposition performance of pure NC and NC/stabilizers mixtures at a specified heating rate, and obtain their decomposition peak temperatures. The compatibility of aziridino[60]fullerene with NC was evaluated by comparing the difference in peak temperature. Under the guidance of NATO-STANAG-4147 standard method, 1.00 mg equal proportion of mixed sample was placed in an aluminum crucible. The test atmosphere was N_2, the flow rate was 50 mL/min, and the heating rate was 10 °C/min. The decomposition peak temperature was recorded and compared with the peak temperature of pure NC. If the exothermic peak temperature increment of the mixed sample is less than 4 °C compared with that of pure NC, they are compatible (Yan et al. 2008).

Methyl violet test

Methyl violet test possesses the superiority of fast, intuitive, and reliability, and it is the conventional method for evaluating the stability of explosives. Under the guidance of GJB-770 B-2005 national military standard method, 300 mg of mixed samples was placed at the bottom of the test tube and in a methyl violet test paper at the distance of 3.0 cm from the surface of the mixed samples. At the test temperature of 134.5 °C, the nitrogen–oxygen acid gas generated by the thermal decomposition of NC changed the methyl violet test paper from purple to orange. The stability of aziridino[60]fullerene to NC was evaluated by discoloration time. The longer the discoloration time, the better the stability.

Vacuum stability test

In VST, a certain amount of sample was heated and decomposed to release gas under constant volume and temperature, and the pressure derived from nitrogen–oxygen acid gas released was detected by a pressure sensor during the measurement. Then, the pressure was converted into the gas volume under the standard state. The larger the gas volume was, the worse the stability performance. In accordance with the GJB-772A-97 standard method, the test temperature was 100 °C, the amount of the samples was 100 mg, and the test time was 48 h. To improve the accuracy and reproducibility, the sample preparation procedure, the amount of sample, and the sensitivity of temperature sensors in the test were strictly controlled. The calculation formula for the gas volume released (V_H) is as follows:

$$V_H = 2.69 \times 10^{-3} \frac{P}{T}(V_0 - V_G) \quad (1)$$

P(Pa) is gas pressure; V_0(mL) is reactor volume; V_G(mL) is sample volume; T(K) is the experimental temperature.

Thermogravimetric test

In the isothermal TG test, an appropriate amount of sample was placed in an aluminum crucible, the sample was kept at a specific temperature for some time and record the thermal weight loss was recorded. The stability performance was evaluated by the weight loss rate of mixed samples. In general, the higher the weight loss rate, the worse the thermal stability. The experiment was guided by the GJB-772A-97 national military standard method. The amount of the samples was 0.75 mg, the test temperature was 135 °C, the atmosphere was N_2, the flow rate was 40 mL/min, and the testing time was 360 min. To improve the accuracy and reproducibility, the sample preparation procedure as well as the amount of sample, heating rate, gas flow rate in the test were strictly controlled.

Electron spin resonance test

The Bruker-EMX nano instrument was used for spectral analysis to determine the ability of aziridino[60] fullerene to scavenge nitroxyl radicals. The central magnetic field was 3373.05 G, the scanning width was 150.0 G, and the g value was 2.0400. SNP (2 mM), $FeSO_4$ (20 mM), DETC (40 mM), and aziridino[60] fullerene of different concentrations (3.2, 1.6, 0.8, 0.4, and 0.2 mM) were oscillated uniformly. After complete mixing, 50 µL of the sample mixture was loaded into glass capillary and then inserted into the capillary scaffold of an ESR spectrometer to record the signal peak intensity. The formula for calculating the free radical clearance rate (X) is as follows:

$$X = \frac{I_0 - I_C}{I_0} \times 100\% \quad (2)$$

I_0 is the ESR signal intensity of the blank sample, and I_c is the ESR signal intensity of NO· after the addition of aziridino[60]Fullerene.

Results and discussion

Characterization

For the structural characterization of **2a–c** and **3a–c**, we have reported in previous work.[46] The structure of products **2d–e** were also characterized by NMR, HRMS, FT-IR, and UV–vis, shown in ESI. In the ^{1}H NMR spectrum of **2e**, the benzene ring exhibits two sets of double peaks at δ 7.57 (d, J=8.34 Hz, 2H) and 7.32 ppm (d, J=8.40 Hz, 2H), and the signal peaks of methyl hydrogen and methylene hydrogen appear individually at δ 2.75 (q, J=7.56 Hz, 2H) and 1.34 (t, J=7.56 Hz, 3H), the integral area ratio is 2:2:2:3. The ^{13}C NMR spectrum of **2e** contains 15 signals derived from the fullerene core. δ 130.58, 128.61, 127.67, and 121.50 ppm are assigned to the benzene ring carbon on the exterior group, 83.75 ppm to the sp^3 carbon on the fullerene carbon cage, and 28.79 and 15.86 ppm to methylene carbon and methyl carbons, respectively. The HRMS of **2e** shows the matching $[M]^-$ ion peak, which confirms the molecular structure. Additionally, corresponding signals may also be observed in the NMR and HRMS spectra of **2d**. The results indicate that we successfully synthesized aziridino[60]fullerenes.

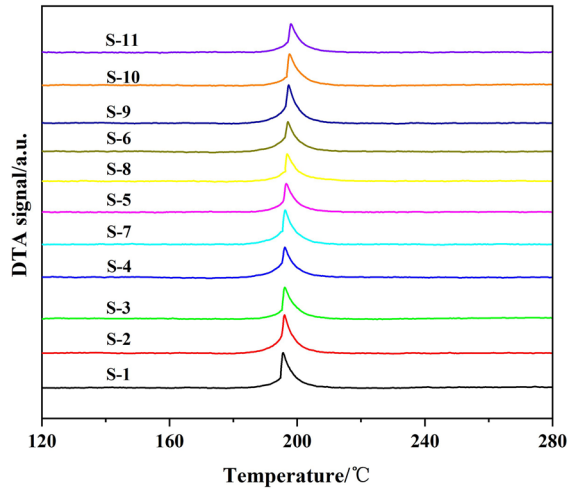

Fig. 1 DTA curves of S-1–S-11

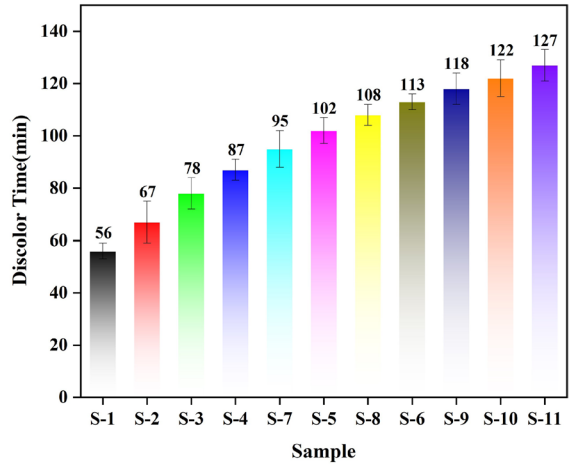

Fig. 2 Discolor time of S-1–S-11

Application of potential nitrocellulose-based propellant stabilizer

Compatibility assessment

As shown in Fig. 1, the DTA curve of pure NC showed that the exothermic peak temperature was 195.58 °C. The exothermic peak temperatures of S-2–S-11 were 196.02, 196.04, 196.13, 196.47, 197.09, 196.26, 196.88, 197.32, 197.53, and 197.95 °C, respectively, which were 0.44, 0.46, 0.55, 0.89, 1.51, 0.68, 1.30, 1.74, 1.95, and 2.37 °C

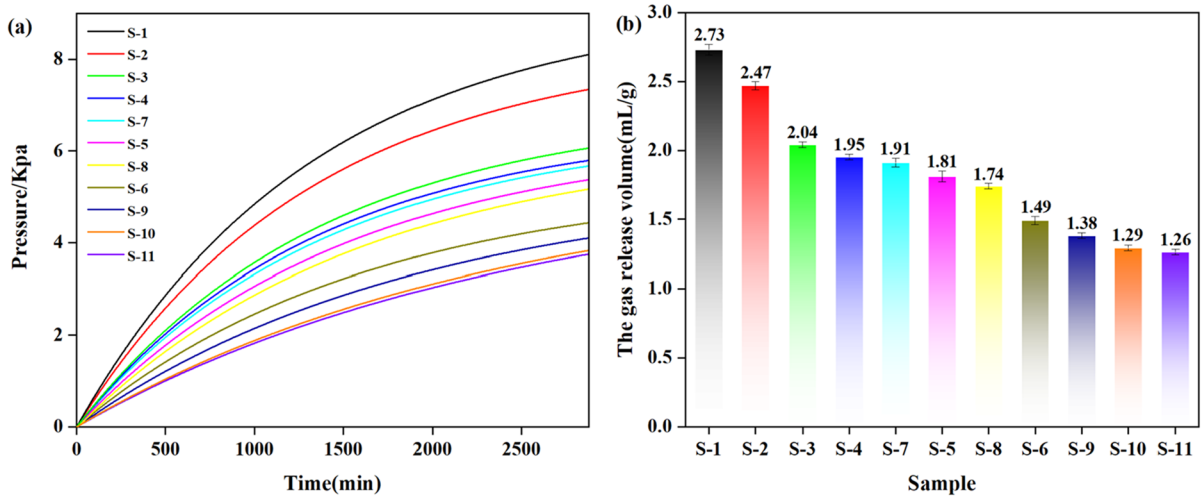

Fig. 3 **a** VST pressure curve of S-1–S-11; **b** Gas release quantity of S-1–S-11

higher than that of pure NC, respectively, indicating that aziridino[60]fullerene has excellent compatibility with NC and the traditional stabilizers DPA and C2.

Methyl violet test

The color change time of S-1–S-11 is shown in Fig. 2. The complete decomposition period of NC was extended by 11–71 min, and the order followed S-11 > S-10 > S-9 > S-6 > S-8 > S-5 > S-7 > S-4 > S-3 > S-2 > S-1. Therefore, the stability of the stabilizers to NC was **3c** > **3b** > **3a** > **2c** > **2e** > **2b** > **2d** > **2a** > C2 > DPA. The experimental results revealed that aziridino[60] fullerene has remarkable stability performance, better than C2 and DPA.

Stability test under vacuum conditions

Under standard conditions, the gas volume was calculated by the transformation equation. The gas volume per unit mass of S-3–S-11 was significantly lower than that of S-1 and S-2, as shown in Fig. 3, at 2.73,

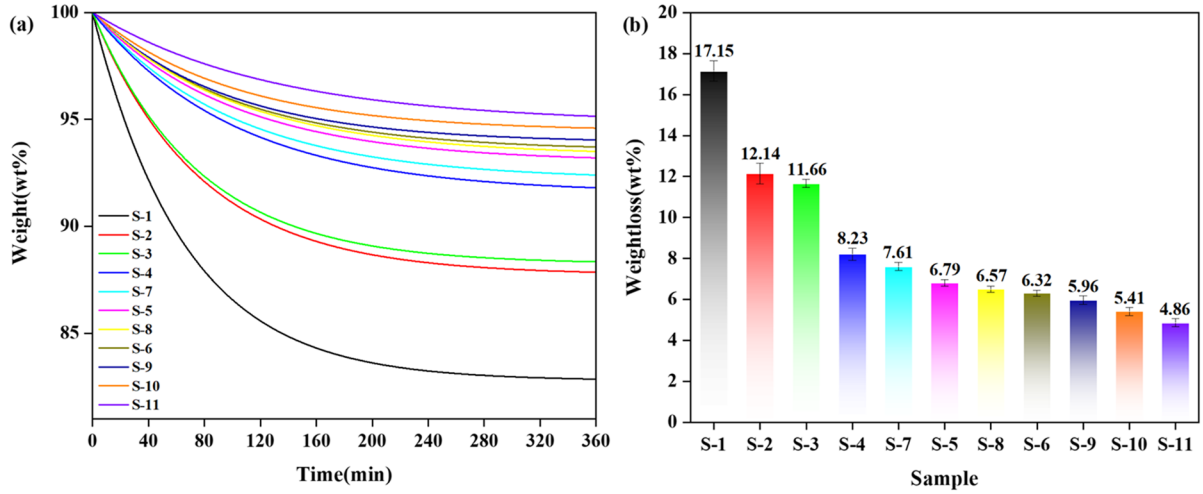

Fig. 4 **a** TG curves of S-1–S-11; **b** Weight loss rate of S-1–S-11

2.47, 2.04, 1.95, 1.91, 1.81, 1.74, 1.49, 1.38, 1.29, and 1.26 mL/g, respectively. The order followed S-11 < S-10 < S-9 < S-6 < S-8 < S-5 < S-7 < S-4 < S-3 < S-2 < S-1. Therefore, the stability of the stabilizers to NC was **3c** > **3b** > **3a** > **2c** > **2e** > **2b** > **2d** > **2a** > C2 > DPA.

Stability test under isothermal conditions

As shown in Fig. 4, the weight-loss rates of S-1–S-11 were 17.15, 12.14, 11.66, 8.25, 6.79, 6.32, 7.61, 6.57, 5.96, 5.41 and 4.86%, respectively. The order followed S-11 < S-10 < S-9 < S-6 < S-8 < S-5 < S-7 < S-4 < S-3 < S-2 < S-1. The weight-loss rate of S-4–S-11 was significantly lower than that of S-1–S-3. Therefore, the stability performance of six stabilizers to NC was in the order **3c** > **3b** > **3a** > **2c** > **2e** > **2b** > **2d** > **2a** > C2 > DPA. The experimental results showed that the addition of aziridino[60]fullerene could improve the heat resistance and stability of NC, obviously superior to traditional stabilizers DPA and C2.

Ability to "capture" to free radicals

The ESR signals of **2a–e** and **3a–c** at different concentrations are depicted in Fig. 5. The strongest ESR signal intensity was detected by the ESR spectrometer in the blank samples, and it was much higher than after adding fullerene derivatives. In addition, the higher the concentration was, the lower the ESR signal intensity. As shown in Fig. 6a, **2a–e** and **3a–c** had different abilities to scavenge nitroxyl radicals at a unified concentration of 3.2 mM, and the order of free-radical scavenging capacity was **3c** > **3b** > **3a** > **2c** > **2e** > **2b** > **2d** > **2a**. The IC50 value was introduced to further determine the free radical scavenging ability. The free-radical scavenging rate of **2a–e** and **3a–c** was fitted at different concentrations (0.2, 0.4, 0.8, 1.6, and 3.2 mM), and the fitting curves are shown in Fig. 6b. The corresponding IC50 value was calculated through the fitting equation when $\eta = 50\%$. The IC50 values of **2a–e** and **3a–c** were 0.92, 0.74, 0.54, 0.87, 0.57, 0.50, 0.43, and 0.24 mM, respectively, and the order followed **3c** > **3b** > **3a** > **2c** > **2e** > **2b** > **2d** > **2a**. The fitting equation and parameters are Eq. (3) and Table 3.

$$\eta = Ae^{\frac{-c}{B}} + T \tag{3}$$

where η (%) is the NO· scavenging rate of aziridino[60]Fullerene and c (mM/L) is the concentration of aziridino[60]Fullerene.

ESR experiment reveals the theoretical feasibility of aziridino[60]fullerenes absorbing nitroxyl radicals. In actual use, aziridino[60]fullerenes may still have some free radicals scavenging ability.

FT-IR test

The reacted fullerene stabilizers were extracted and analyzed by FT-IR after the reaction of **3a** with the nitrogen oxides generated through the thermal degradation of NC, and changes in their functional groups were preliminarily detected. As depicted in Fig. 7, the symmetric and asymmetric vibrational peaks of $-NO_2$ are positioned approximately 1272 cm^{-1} and 1637 cm^{-1}, respectively. Furthermore, the C–N extended vibrational peak is found about 825 cm^{-1}, and the C–N–O bent vibrational peak is found near 744 cm^{-1}. These observations tentatively suggested that **2d** interracts with nitrogen oxides chemically.

Conclusion

In conclusion, four mono-aziridino[60]fullerenes were synthesized and characterized by NMR, HRMS, FT-IR, UV–vis, and X-ray single-crystal diffraction. DTA, methyl violet, VST, and TG test were introduced to evaluate the compatibility and stability of aziridino[60]fullerene to NC. The experimental results revealed that aziridino[60]fullerene had better thermal stability than C2 and DPA. Furthermore, the ability of aziridino[60]fullerene to absorb nitroxyl radicals was studied by ESR. The higher the concentration was, the stronger the absorption capacity. When the concentration was 3.2 mM, the free-radical scavenging rate of **3c** reached 86.09%. These results revealed that aziridino[60]fullerene could effectively scavenge nitroxyl radicals, and the longer the carbon chain of the external group, the stronger the ability to absorb free radicals. Fullerene-based stabilizers have

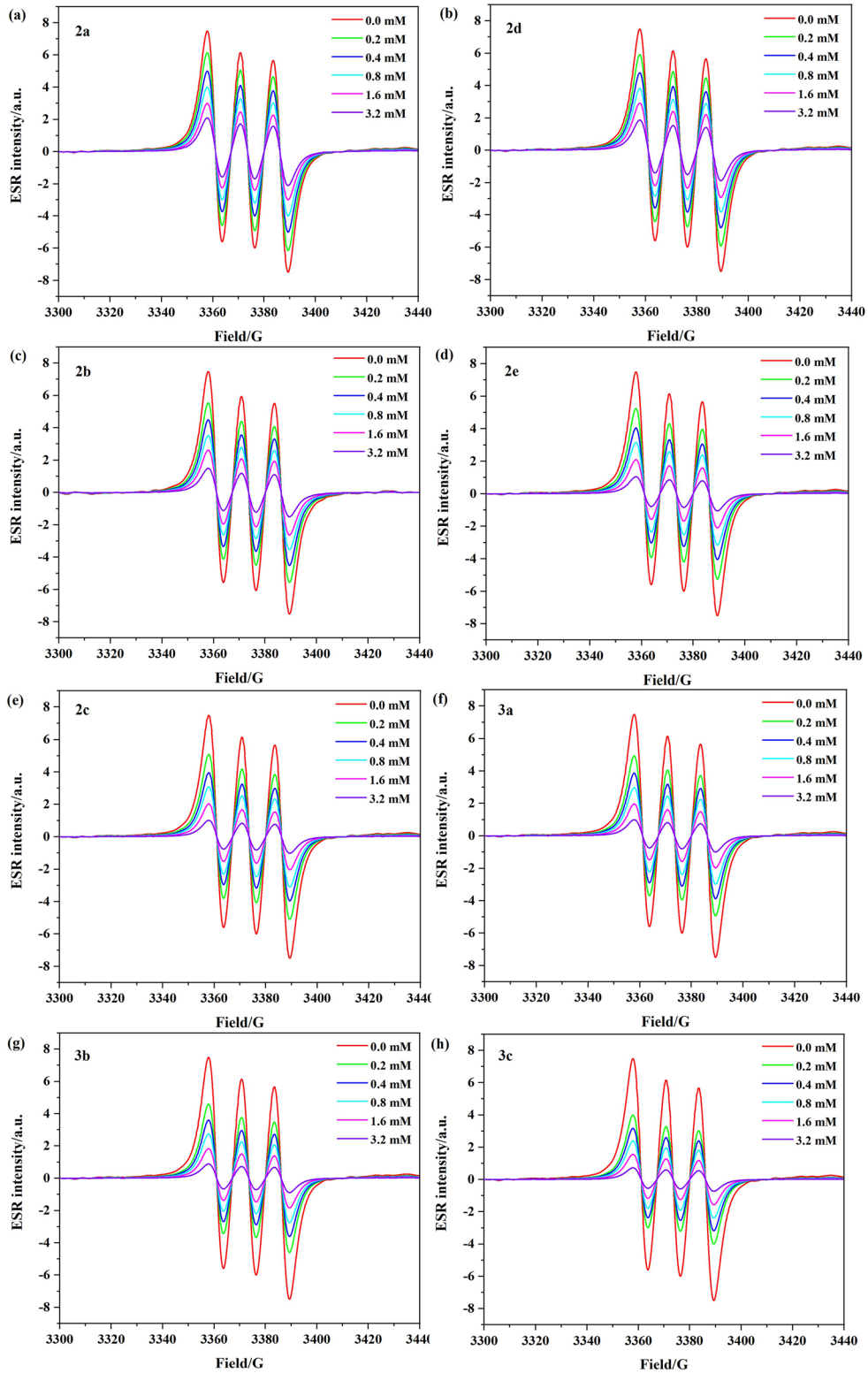

Fig. 5 ESR signals of NO scavenging of **2a–e** and **3a–c**

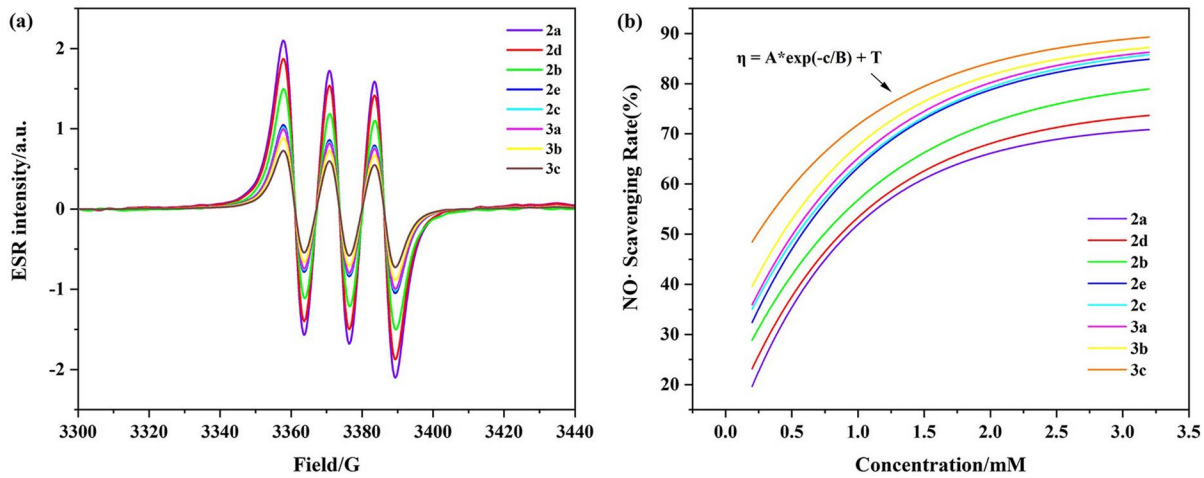

Fig. 6 **a** ESR signals of aziridino[60]fullerene at 3.2 mM; **b** fitting curves of the NO· scavenging rates

Table 3 Fitting parameters of the aziridino[60]Fullerene at different concentrations for NO· scavenging rates

Fullerene derivatives	A	B	C	R^2
2a	−66.81	0.84	72.36	0.99
2b	−64.25	1.08	82.26	0.99
2c	−65.14	1.04	88.09	0.97
2d	−65.17	0.94	75.85	0.99
2e	−67.59	0.97	87.39	0.99
3a	−64.74	0.99	99.79	0.98
3b	−61.36	0.96	89.43	0.98
3c	−52.47	1.02	91.62	0.98

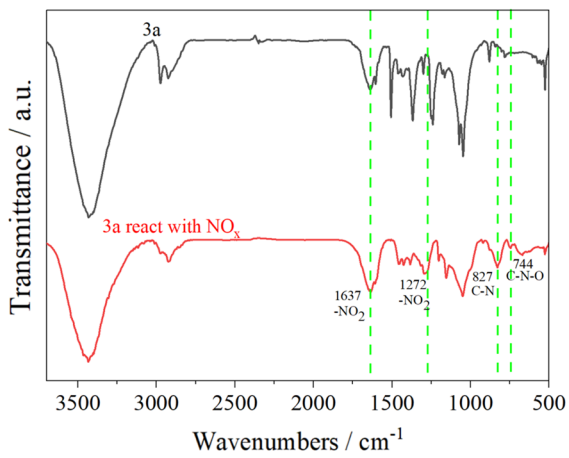

Fig. 7 FT-IR spectra of **3a** after and before interaction with NC

a distinctive ability to scavenge free radicals compared to other stabilizers, such as zeolites, organic eutectics. Therefore, applying bifunctional fullerene derivatives to the field of stabilizers is of great importance.

Experimental characterization data

The structures of the **2a–c** and **3a–c** were previously reported, and the structural characterisation data for the **2d–e** are as follows:

2d: ^{1}H NMR (600 MHz, CS_2–$CDCl_3$) δ 7.53 (d, J = 8.28 Hz, 2H), 7.28 (d, J = 7.98 Hz, 2H), 2.45 (s, 3H); ^{13}C NMR (150 MHz, CS_2–$CDCl_3$) δ 145.30, 145.21, 144.98, 144.88, 144.79, 144.63, 144.17, 143.94, 142.92, 142.34, 142.27, 142.05, 141.01, 140.79, 133.62(Ar–C), 130.29(Ar–C), 129.86(Ar–C), 121.55(Ar–C), 83.76(sp^3-C), 21.32(Alkyl-C); HRMS (MALDI-TOF) m/z: M^- calcd for $C_{67}H_7N$ 825.0578, found 825.0571.

2e: ^{1}H NMR (600 MHz, CS_2–$CDCl_3$) δ 7.57 (d, J = 8.34 Hz, 2H), 7.32 (d, J = 8.40 Hz, 2H), 2.75 (q, J = 7.56 Hz, 2H), 1.34 (t, J = 7.56 Hz, 3H); ^{13}C NMR (150 MHz, CS_2–$CDCl_3$) δ 145.29, 145.20, 145.01, 144.86, 144.79, 144.63, 144.15, 143.93, 143.34, 142.91, 142.35, 142.25, 140.99, 140.78, 139.95, 130.58(Ar–C), 128.61(Ar–C), 127.67(Ar–C), 121.50(Ar–C), 83.75(sp^3-C), 28.79(Alkyl-C), 15.86(Alkyl-C); HRMS (MALDI-TOF) m/z: M^- calcd for $C_{68}H_9N$ 839.0735, found 839.0731.

Acknowledgments We are grateful for financial support from the Natural Science Foundation of China (Project No. 51972278), Outstanding Youth Science and Technology Talents Program of Sichuan (No. 19JCQN0085), and Open Project of State Key Laboratory of Environment-friendly Energy Materials (Southwest University of Science and Technology, No. 22fksy18).

Author contributions JX and SF jointly completed all experimental parts and the main thesis writing. Prof. RP and Prof. BJ provided project support and experimental guidance for the work, and revised the paper. All authors read and approved the final manuscript.

Funding This research did not receive any specific grant from funding agencies in the public, commercial, or not-for-profit sectors.

Data availability All data generated or analysed during this study are included in this published article.

Declarations

Conflict of interest The authors declare no competing interests.

Ethics approval and consent to participate The authors are compliance with ethical standards.

Consent for publication Written informed consent for publication was obtained from all participants.

References

Asthana SN, Divekar CN, Singh H (1989a) Studies on thermal stability, autoignition and stabilizer depletion for shelf life of CMDB propellants. J Hazard Mater 21:35–46

Asthana SN, Deshpande BY, Singh H (1989b) Evaluation of various stabilizers for stability and increased life of CMDB propellants. Propellants Explos Pyrotech 14:170–175

Ahmed FT, Djalal T, Thomas MK, Burkhard K (2020) New insensitive nitrogen-rich energetic polymers based on amino-functionalized cellulose and microcrystalline cellulose: Synthesis and characterization. Fuel 277:118258–118272

Ahmed FT, Djalal T, Mohamed AH, Amir A, Hani B, Imene C, Sabri T, Thomas MK (2023) Elucidating the characteristics of a promising nitrate ester polysaccharide derived from shrimp shells and its blends with cellulose nitrate. Cellulose 30:4941–4955

Bohn MA (2009) Prediction of in-service time period of three differently stabilized single base propellants. Propellants Explos Pyrotech 34:252–266

Birkett PR, Hitchcock PB, Kroto HW, Taylor R, Walton DRM (1992) Preparation and characterization of $C_{60}Br_6$ and $C_{60}Br_8$. Nature 357:479–481

Bagalkote V, Grinstein D, Natan B (2018) Energetic nanocomposites as burn rate catalyst for composite solid propellants. Propellants Explos Pyrotech 43:136–143

Closs GL, Gautam P, Zhang D, Krusic PJ, Hill SA, Wasserman E (1992) Steady-state and time-resolved direct detection EPR spectra of fullerene triplets in liquid solution and glassy matrixes: evidence for a dynamic Jahn-Teller effect in triplet C_{60}. J Phys Chem 96:5228–5231

Chai H, Duan Q, Jiang L, Gong L, Chen H, Sun J (2019) Theoretical and experimental study on the effect of nitrogen content on the thermal characteristics of nitrocellulose under low heating rates. Cellulose 26:763–776

Chelouche S, Trache D, Tarchoun AF, Abdelaziz A, Khimeche K, Mezroua A (2019) Organic eutectic mixture as efficient stabilizer for nitrocellulose: kinetic modeling and stability assessment. Thermochim Acta 673:78–91

Chai ZH, Luo LQ, Jin B, Zhao Y, Xiao LPC, Li G, Ding L, Zhang QC, Peng RF (2020) Fullerene stabilizer 4,11,15,30-tetraarylamino fullerenoarylaziridine: regioselective synthesis, crystallographic characterization derivatives, and potential application as propellant stabilizer. ACS Appl Energy Mater 3:3005–3014

Drzyzga O (2003) Diphenylamine and derivatives in the environment: a review. Chemosphere 53:809–818

de Klerk WPC (2015) Assessment of stability of propellants and safe lifetimes. Propellants Explos Pyrotech 40:388–393

Ding L, Jin B, Guo ZC, Zhao Y, Chen JJ, Peng RF (2019) Regioselective synthesis and crystallographic characterization of nontethered *cis-1* and *cis-2* Bis(benzofuro)[60] fullerene derivatives. Org Lett 21:9924–9928

Elbasuney S, Fahd A, Mostafa HE, Mostafa SF, Sadek R (2018) Chemical stability, thermal behavior, and shelf life assessment of extruded modified double-base propellants. Def Technol 14:70–76

Ishida H, Komori K, Itoh K, Ohno M (2000) Diels-Alder reaction of [60]fullerene with cyclooctatetraene and electrophilic addition to the cycloadduct. Tetrahedron Lett 41:9839–9842

Jin B, Shen J, Peng RF, Chen C, Zhang QC, Wang X, Chu SJ (2015) DMSO: an efficient catalyst for the cyclopropanation of C_{60}, C_{70}, SWNTs, and graphene through the bingel reaction. Ind Eng Chem Res 54:2879–2885

Krumlinde P, Ek S, Tunestål E, Hafstrand A (2017) Synthesis and characterization of novel stabilizers for nitrocellulose-based propellants. Propellants Explos Pyrotech 42:78–83

Krusic PJ, Wasserman E, Keizer PN, Morton JR, Preston KF (1991) Radical reactions of C_{60}. Science 254:1183–1185

Katoh K, Yoshino S, Kubota S, Wada Y, Ogata Y, Nakahama M, Kawaguchi S, Arai M (2007) The effects of conventional stabilizers and phenol compounds used as antioxidants on the stabilization of nitrocellulose. Propellants Explos Pyrotech 32:314–321

Lindblom T (2002) Reactions in stabilizer and between stabilizer and nitrocellulose in propellants. Propellants Explos Pyrotech 27:197–208

Li CZ, Yip HL, Jen AKY (2012) Functional fullerenes for organic photovoltaics. J Mater Chem 22:4161–4177

Li G, Jin B, Chai ZH, Ding L, Chu SJ, Peng RF (2020a) Synthesis and crystal characterization of novel fulleropyrrolidines and their potential application as

nitrocellulose-based propellants stabilizer. Polym Degrad Stabil 172:109061

Li G, Jin B, Chai ZH, Liao L, Chu SJ, Peng RF (2020b) Synthesis and stabilization mechanism of novel stabilizers for fullerene-malonamide derivatives in nitrocellulose-based propellants. Polym Test 86:106493

Liao L, Jin B, Guo ZC, Xian F, Hou CJ, Peng RF (2021) Fullerene bisadduct stabilizers: the effect of different addition positions on inhibiting the autocatalytic decomposition of nitrocellulose absorbed nitroglycerin. Def Technol 17:1944–1953

Luo LQ, Jin B, Chai ZH, Huang Q, Chu SJ, Peng RF (2019a) Interaction and mechanism of nitrocellulose and N-methyl-4-nitroaniline by isothermal decomposition method. Cellulose 26:9021–9033

Luo LQ, Jin B, Xiao YY, Zhang QC, Chai ZH, Huang Q, Chu SJ, Peng RF (2019b) Study on the isothermal decomposition kinetics and mechanism of nitrocellulose. Polym Test 75:337–343

Lussier LS, Gagnon H, Bohn MA (2000) On the chemical reactions of diphenylamine and its derivatives with nitrogen dioxide at normal storage temperature conditions. Propellants Explos Pyrotech 25:117–125

Lussier LS, Bergeron E, Gagnon H (2006) Study of the daughter products of Akardite-II. Propellants Explos Pyrotech 31:253–262

McEwen CN, McKay RG, Larsen BS (1992) C_{60} as a radical sponge. J Am Chem Soc 114:4412–4414

Memdouh C, Fouad B, Djalal T, Amir A, Ahmed FT (2023) Insight into the stability and thermal decomposition behavior of nitrocellulose supplemented with different types of zeolites. Propellants Explos Pyrotech 48:e202300091

Mohamed FC, Djalal T, Fouad B, Ahmed FT, Salim C, Abderrahmane M (2020) Organosolv lignins as new stabilizers for cellulose nitrate: thermal behavior and stability assessment. Int J Biol Macromol 164:794–807

Montellano A, Da RT, Bianco A, Prato M (2011) Fullerene C_{60} as a multifunctional system for drug and gene delivery. Nanoscale 3:4035–4041

Nassima S, Amir A, Ahmed FT, Hani B, Abderahmane M, Djalal T (2022) Nitrostarch as a promising insensitive energetic biopolymer: Synthesis, characterization, and thermal decomposition kinetics. Ind Crops Prod 189:115774–115783

Prato M (1997) [60]Fullerene chemistry for materials science applications. J Mater Chem 7:1097–1109

Purves CB, Grassie VR, Mitchell L, Pepper JM (1950) Preliminary tests on possible new stabilizers for nitrocelluloses. Can J Res 28b:468–484

Sabri T, Moulai KB, Djalal T, Elamine L, Hamdane A, Samir B, Manel N (2023) Dual influence of nano barium oxide on thermal decomposition reaction kinetics and chemical stability of cellulose nitrate. Cellulose 30:5503–5518

Salim C, Djalal T, Catarina MSSN, Simao PP, Kamel K, Mokhtar B (2018) Solid + liquid equilibria and molecular structure studies of binary mixtures for nitrate ester's stabilizers: Measurement and modeling. Thermochim Acta 666:197–207

Taylor R, Walton DRM (1993) The chemistry of fullerenes. Nature 363:685–693

Trache D, Tarchoun AF (2018) Stabilizers for nitrate ester-based energetic materials and their mechanism of action: a state-of-the-art review. J Mater Sci 53:100–123

Trache D, Tarchoun AF (2019) Analytical methods for stability assessment of nitrate esters-based propellants. Crit Rev Anal Chem 49:415–438

Tang Q, Fan X, Li J, Bi F, Fu X, Zhai L (2017) Experimental and theoretical studies on stability of new stabilizers for N-methyl-P-nitroaniline derivative in CMDB propellants. J Hazard Mater 327:187–196

Troshin PA, Kolesnikov D, Burtsev AV, Lubovskaya RN, Denisenko NI, Popov AA, Troyanov SI, Boltalina OV (2003) Bromination of [60]fullerene. I. High-yield synthesis of $C_{60}Br_x$ (x=6, 8, 24). Fuller Nanotub Carbon Nanostruct 11:47–60

Troshin PA, Kemnitz E, Troyanov SI (2004) Characterization of reactions of fullerene C_{60} with bromine. Crystal structures of bromofullerenes $C_{60}Br_6$, $C_{60}Br_6{\cdot}CS_2$, $_{C6}0B_t8{\cdot}CHB_t3{\cdot}2B_t2$, and $_{C6}0B_{t2}4{\cdot}_{C}6_H4C_l2{\cdot}B_t2$. Russ Chem Bull 53:2787–2792

Vennerstrom JL, Holmes TJ (1987) Prostaglandin-H synthase inhibition by malonamides. Ring-opened analogs of phenylbutazone. J Med Chem 30:434–437

Wilker S, Heeb G, Vogelsanger B, Petržílek J, Skládal J (2007) Triphenylamine—a 'New' stabilizer for nitrocellulose based propellants—part i: chemical stability studies. Propellants Explos Pyrotech 32:135–148

Xiao YF, Wang AQ, Liu Y, Liu XM, Yao ZQ (1994) Langmuir-Blodgett film of 1,3,6,11,13,18,28,31-octabromofullerene-C_{60}. Thin Solid Films 251:4–6

Xiong J, Feng S, Peng RF, Jin B (2023) Stereoselective synthesis of nontethered *trans-4* Bis(aziridino)[60]fullerene derivatives. Chin J Chem 41:2282–2288

Yan QL, Xiao JL, La YZ, Ji ZL, Hong LL, Zi RL (2008) Compatibility study of *trans*-1,4,5,8-tetranitro-1,4,5,8-tetraazadecalin (TNAD) with some energetic components and inert materials. J Hazard Mater 160:529–534

Yan QL, Gozin M, Zhao FQ, Cohen A, Pang SP (2016) Highly energetic compositions based on functionalized carbon nanomaterials. Nanoscale 8:4799–4851

Zhao FQ, Heng SY, Hu RZ, Gao HX, Fang H (2007) A study of kinetic behaviours of the effective centralite/stabilizer consumption reaction of propellants using a multi-temperature artificial accelerated ageing test. J Hazard Mater 145:45–50

Zayed MA, El-Begawy SEM, Hassan HES (2017) Mechanism study of stabilization of double-base propellants by using zeolite stabilizers (nano- and micro-clinoptilolite). Arab J Chem 10:573–581